Statistics of light-ion-induced kinetic electron emission: The sum of Poisson distribution

Martin Vicanek and Herbert M. Urbassek
Institut für Theoretische Physik, Technische Universität, W-3300 Braunschweig, Germany
(Received 21 August 1992; revised manuscript received 11 November 1992)

A model on the statistics of ion-induced kinetic electron emission is presented. The model is primarily designed to describe light-ion bombardment at energies not too far above the threshold for kinetic-electron emission. We use an invariant-embedding approach, which includes angular scattering and stopping of the ion, electron excitation, and elastic and inelastic scattering. A particularly simple picture evolves when the ion travels on a straight line in the vicinity of the surface: Then the emission statistics is simply a sum of two Poisson distributions, where the ion reflection coefficient determines the weight of the Poisson terms. Comparison to experiment is favorable. Extensions with respect to ion trajectory, energy dependence, and recoil contribution are discussed.

I. INTRODUCTION

When a solid surface is bombarded by energetic ions, secondary electrons may be emitted.[1–5] The potential energy set free when the ion is neutralized may lead to *potential* electron emission. In the present article, however, we shall be interested in *kinetic* electron emission in which the kinetic energy of the bombarding ion is used to emit electrons from the solid. This mechanism is active if the ion energy exceeds a threshold. Already, some time ago, the statistics of electron emission was measured.[6–8] Interest in this question stems in particular from the needs of single-particle counting with ion-electron converters and secondary electron multipliers. Quite recently, measurements of emission statistics could be extended to much lower ion energies.[9–12] These data were used to obtain information on the threshold behavior of kinetic emission, and thus a clear distinction of potential and kinetic emission in the threshold regime was obtained.

Existing theories of ion-induced electron emission view the phenomenon as a three-step process:[3,4,13–18] (i) generation of energetic electrons inside the target, (ii) transport of electrons to the surface, and (iii) escape of electrons into the vacuum. The main differences between the existing theories lie in the level of sophistication with which the individual steps are incorporated. Thus, in the first step, electron excitation may occur in direct collisions of the ion with conduction or valence electrons, by the ionization of target inner shells, and for fast heavy ions, by electron loss from the projectile. A number of secondary processes may also contribute to electron excitation, such as electron cascade multiplication, recoil ionization, and plasmon decay. In the second step, excited electrons usually undergo a sequence of elastic and inelastic collisions with the target ionic cores and electrons, respectively, before some of them may reach the surface. In its simplest form, this transport process is modeled as an exponential attenuation.[13–15] In the third step, electrons must overcome the surface barrier in order to escape into the vacuum. This process is important for the energy spectrum of emitted electrons.[3]

So far, existing theories have been used to calculate *average* quantities such as, for instance, the mean electron yield γ. In this article we present a model of the statistics of ion-induced kinetic electron emission. We shall focus on *light-ion* bombardment with energies not too far above threshold. In this case, target atoms will recoil with comparatively small energies in collisions with the projectile ion, and hence the contribution of recoil atoms to kinetic electron emission can be safely disregarded; this simplifies the analysis considerably. Furthermore, the multiplication of secondary electrons in electron cascades can be disregarded. We note that similar considerations apply for all projectile ions in the threshold regime.

The basic idea of this paper is that the ion excites secondary electrons along its trajectory in statistically independent events. The probability that exactly n electrons make it to the surface and are emitted thus obeys a Poisson distribution with average γ,

$$P_n(\gamma)=\frac{\gamma^n}{n!}e^{-\gamma} . \tag{1}$$

However, different ions will move along different trajectories, and to each trajectory belongs an individual value of γ. Hence, ions which stay longer in a near-surface region where excited electrons have a good chance to be emitted will be characterized by a larger average electron yield γ.

A great simplification results if the length scale for the ion motion is much larger than the corresponding length scale for the secondary electrons. In this case, only two classes of ion trajectories need to be distinguished, namely, those where the ion is implanted and those which lead to reflection. The respective average yields may be denoted by γ_0 and γ_1, and the probability W_n that exactly n secondary electrons are emitted is given by a weighted sum of Poissonians,

$$W_n=(1-R)P_n(\gamma_0)+RP_n(\gamma_1) , \tag{2}$$

where R is the ion reflection coefficient.

 ©1993 The American Physical Society

The main part of the present paper serves to justify the sum of Poisson distribution. Indeed, its *ad hoc* formulation leaves a number of questions open. While the *excitation* process can be described by Poisson distributions, not all excited electrons are actually emitted, and we may wonder whether the above distribution also applies to *emitted* electrons. Furthermore, if the average yields γ_0 and γ_1 are not simply to be regarded as fit parameters to be obtained from experiment, one would like to obtain a microscopic interpretation in terms of the electron excitation, and elastic- and inelastic-scattering cross sections. Finally, one needs to discuss the limits of this model in order to delineate its regime of validity more clearly.

In Sec. II we shall give a quantitative formulation of this model, based on an invariant-embedding approach formulation. This approach allows one in particular to calculate the parameters entering the Poisson distributions as a function of the microscopic elastic- and inelastic-scattering cross sections of the electrons. In Sec. III the limitations of the approach are discussed, and its results are compared to experiment. Section IV serves to discuss several extensions and generalizations of the sum of Poisson distributions model towards higher ion mass and bombarding energy.

II. THE SUM OF POISSON DISTRIBUTIONS MODEL: INVARIANT EMBEDDING

In this section we present a transport theoretic derivation of the sum of Poisson distributions. This will allow us to express the average yields γ_0 and γ_1 in terms of microscopic electron excitation and scattering cross sections. We shall use the technique of invariant embedding[19–21] for this purpose.

We include the following microscopic processes: The electron excitation cross section σ_x of the ion and the number density N of the target define the probability that the ion excites an electron while traveling a path length Δx as $\Delta x N \sigma_x$. Since, in particular near threshold, a correlation between the directions of the exciting ion $\mathbf{\Omega}_i$ and the excited electron $\mathbf{\Omega}_e$ may exist, we write $\sigma_x = \sigma_x^+ + \sigma_x^-$, where σ_x^+ is the cross section for exciting an electron in the direction of the ion ($\mathbf{\Omega}_i \mathbf{\Omega}_e > 0$), and σ_x^- in the opposite direction. Furthermore, we need the inelastic-scattering cross section σ_{in}, which describes the stopping of electrons; it is connected to the average range Z of electrons via $Z = 1/N\sigma_{\text{in}}$. The reversal of the direction of flight of the electrons is characterized by the elastic-scattering cross section σ_{el}. This quantity is connected to the well-known transport mean free path λ_{tr}, which denotes the length that a monodirectional beam of electrons needs to travel until it is isotropized; it is $\lambda_{\text{tr}} = 1/2N\sigma_{\text{el}}$.

In this section the only information used to describe the ion transport is contained in the reflection coefficient R. The elastic and inelastic scattering of the ion can be included to obtain a complete coupled description of electron and ion transport. This will be presented in Sec. IV A below.

It turns out that it is not possible to write down equations for the probabilities W_n directly. Rather, one must study the joint probabilities W_n^0 (W_n^1) that exactly n electrons are emitted *and* that the ion is stopped in the target (reflected from the target). Since the ion must suffer exactly one of these two fates, it is

$$W_n = W_n^0 + W_n^1 \ . \tag{3}$$

Let us first set up an equation for W_n^0. We shall use a one-dimensional approach in which particle motion is distinguished only between moving into or out of the target. Furthermore, the energy dependence of the various cross sections will be disregarded, and we shall only distinguish between moving and stopped particles.

The invariant-embedding argument goes as follows: The probability W_n^0 that exactly n electrons are emitted cannot change if a layer of a small depth Δx is added to the target surface. In this layer, however, the following processes can occur (cf. Fig. 1).

(1) The ion excites with probability $N\sigma_x^- \Delta x$ an electron in the layer Δx which travels towards the surface and is emitted. This process contributes to W_n^0 only if $n-1$ electrons had been emitted without the layer Δx introduced. Hence, the contribution reads

$$N\sigma_x^- \Delta x W_{n-1}^0 \ . \tag{4}$$

(2) The ion excites with probability $N\sigma_x^+ \Delta x$ an electron in layer Δx which travels into the target. The electron is reflected with probability R_e. This process contributes

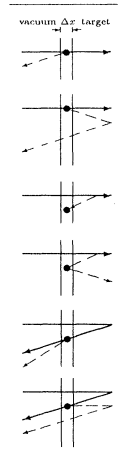

process	+gain / −loss } to W_n^0	+gain / −loss } to W_n^1
	$+N\sigma_x^- \Delta x W_{n-1}^0$ $-N\sigma_x^- \Delta x W_n^0$	$+N\sigma_x^- \Delta x W_{n-1}^1$ $-N\sigma_x^- \Delta x W_n^1$
	$+N\sigma_x^+ \Delta x R_e W_{n-1}^0$ $-N\sigma_x^+ \Delta x R_e W_n^0$	$+N\sigma_x^+ \Delta x R_e W_{n-1}^1$ $-N\sigma_x^+ \Delta x R_e W_n^1$
	$+(n+1)N\sigma_{\text{in}} \Delta x W_{n+1}^0$ $-nN\sigma_{\text{in}} \Delta x W_n^0$	$+(n+1)N\sigma_{\text{in}} \Delta x W_{n+1}^1$ $-nN\sigma_{\text{in}} \Delta x W_n^1$
	$+(n+1)N\sigma_{\text{el}} \Delta x (1-R_e) W_{n+1}^0$ $-nN\sigma_{\text{el}} \Delta x (1-R_e) W_n^0$	$+(n+1)N\sigma_{\text{el}} \Delta x (1-R_e) W_{n+1}^1$ $-nN\sigma_{\text{el}} \Delta x (1-R_e) W_n^1$
	0	$+N\sigma_x^+ \Delta x W_{n-1}^1$ $-N\sigma_x^+ \Delta x W_n^1$
	0	$+N\sigma_x^- \Delta x R_e W_{n-1}^1$ $-N\sigma_x^- \Delta x R_e W_n^1$

FIG. 1. Processes contributing in a surface layer of depth Δx to the joint probability W_n^0 (W_n^1) that exactly n electrons are ejected *and* that the bombarding ion is stopped in the target (reflected from the target). In this simplified discussion (Sec. II), only the electron excitation cross sections σ_x^+ and σ_x^-, the elastic-scattering cross section σ_{el}, and the inelastic-scattering cross section σ_{in} of the electron enter. The icons are meant to give a pictorial representation of the processes. Solid (dashed) lines denote ion (electron) trajectories, and the dot represents a collision event in the layer Δx.

$$N\sigma_x^+ \Delta x R_e W_{n-1}^0 \ . \tag{5}$$

The electron reflection coefficient R_e can be expressed in terms of $\sigma_{\rm el}$ and $\sigma_{\rm in}$; see Eq. (19) below.

(3) One of the electrons excited in the target may be stopped in the layer Δx (probability $N\sigma_{\rm in}\Delta x$). This process contributes only if exactly $(n+1)$ electrons have reached the surface layer. This process contributes

$$(n+1)N\sigma_{\rm in}\Delta x W_{n+1}^0 \ . \tag{6}$$

(4) One of the electrons excited in the target is reflected back into the target (probability $N\sigma_{\rm el}\Delta x$). This process contributes only if $(n+1)$ electrons have reached the target surface, and the electron reflected in Δx is not reflected back in the target towards the surface. This process contributes

$$(n+1)N\sigma_{\rm el}\Delta x(1-R_e)W_{n+1}^0 \ . \tag{7}$$

Finally, there is a probability that none of the above processes occurs in Δx, which contributes

$$[1-N\sigma_x^-\Delta x - N\sigma_x^+\Delta x R_e - nN\sigma_{\rm in}\Delta x - nN\sigma_{\rm el}\Delta x(1-R_e)]W_n^0 \ . \tag{8}$$

Balancing W_n^0 with the sum of Eqs. (4)–(8), we obtain

$$0=\frac{n+1}{L_{\rm esc}}W_{n+1}^0-\left[\frac{1}{L_x^0}+\frac{n}{L_{\rm esc}}\right]W_n^0+\frac{1}{L_x^0}W_{n-1}^0 \ , \tag{9}$$

where the backward excitation length of an ion which is stopped in the target

$$L_x^0=1/N(\sigma_x^-+\sigma_x^+R_e) \tag{10}$$

and the escape length of the electrons

$$L_{\rm esc}=1/N[\sigma_{\rm in}+(1-R_e)\sigma_{\rm el}] \tag{11}$$

have been introduced.

An analogous equation can be set up for W_n^1. As Fig. 1 shows, in this case two more processes contribute. The resulting balance equation looks identical to Eq. (9), if L_x^0 is replaced by the excitation length of a reflected ion:

$$L_x^1=1/N[(\sigma_x^-+\sigma_x^+)(1+R_e)] \ . \tag{10'}$$

We note that $1/L_x^1=1/L_x^0+1/L_x^+$, where

$$L_x^+=1/N(\sigma_x^++\sigma_x^-R_e) \tag{12}$$

is the forward excitation length of the ion.

Since the Poisson distribution $P_n(\gamma)$ obeys the recursion relation

$$nP_n(\gamma)-\gamma P_{n-1}(\gamma)=0 \ , \tag{13}$$

Eq. (9) and its analog for W_n^1 are solved by

$$W_n^0=(1-R)P_n(\gamma_0) \ , \quad W_n^1=RP_n(\gamma_1) \ . \tag{14}$$

The prefactors stem from the normalization

$$\sum_{n=0}^{\infty} W_n^0=1-R \ , \quad \sum_{n=0}^{\infty} W_n^1=R \ . \tag{15}$$

Thus, we have derived the sum of Poisson distributions, Eq. (2). The mean values

$$\gamma_{0,1}=L_{\rm esc}/L_x^{0,1} \tag{16}$$

denote the mean number of electrons excited in a near-surface layer of the extent of an electron escape length under the condition that the ion is stopped or reflected, respectively, in the target.

III. DISCUSSION

Let us denote the average yield by γ. It is

$$\langle n\rangle=\gamma=(1-R)\gamma_0+R\gamma_1 \ . \tag{17}$$

The variance of the distribution (2) is

$$\sigma^2=\langle n^2\rangle-\langle n\rangle^2=\gamma+R(1-R)(\gamma_1-\gamma_0)^2>\langle n\rangle \ . \tag{18}$$

Evidently, the variance of the sum of Poisson distribution is larger than that of a single Poisson distribution. Fluctuations of the fate of the ion add to the fluctuations in the electron-yield statistics.

Recently, Monte Carlo simulations were performed to model the statistics of kinetic electron emission from ion-bombarded solids.[22] For light-ion bombardment, their results showed that deviations from Poisson statistics are due to backscattered ions. This conclusion is in agreement with our study.

Our result, Eq. (2), contains three parameters. Two of them, viz., R and γ, are experimentally well known. The third parameter, which may be chosen as $\gamma_1-\gamma_0$, may either be regarded as a fit parameter to be determined from experiment, which is easiest done using Eq. (18), or may be determined from theory [cf. Eqs. (10), (11), and (16)].

Within the present model, the electron reflection coefficient can be expressed in terms of the elastic and inelastic cross sections as

$$R_e=1+\frac{\sigma_{\rm in}}{\sigma_{\rm el}}-\left[\frac{\sigma_{\rm in}}{\sigma_{\rm el}}\left[\frac{\sigma_{\rm in}}{\sigma_{\rm el}}+2\right]\right]^{1/2} \ . \tag{19}$$

This relation may be derived in a straightforward way from an invariant-embedding argument. Inserting Eq. (19) into Eq. (11) yields the electron escape length as

$$1/L_{\rm esc}=N\sqrt{\sigma_{\rm in}(\sigma_{\rm in}+2\sigma_{\rm el})} \ . \tag{11'}$$

Thus, for negligible elastic scattering, the escape length is equal to the average range of electrons, $1/N\sigma_{\rm in}$, whereas it becomes smaller for non-negligible elastic scattering. Expressions for the two limiting cases of weak and strong elastic scattering, respectively, have been derived before;[18] these agree—apart from a numerical factor—with the corresponding limits of Eq. (11′).

The model makes a number of assumptions.

(i) The invariant-embedding approach adopted here treats the direction of motion of the ion and of the excited electrons in the target in a rather schematical way. In principle, this restriction can be given up at the price of obtaining a system of integral equations instead of the algebraic system (9). This issue will not be studied further here.

(ii) The ion is assumed to travel on a straight line in the vicinity of the surface. If stopping and angular scattering of the ion in the surface layer are important, deviations from the Poisson law (14) will occur. This is only of minor importance for light-ion bombardment and will be discussed further in Sec. IV A.

(iii) The energy of the reflected ions does not enter in the simple model presented above, although one might argue that an ion reflected with higher energy will excite more electrons on its way towards the surface than at lower energies. Extensions in this respect are discussed in Sec. IV B.

(iv) Recoil atoms energized by the light ion do not contribute to kinetic electron emission. This restricts the validity of the model to light-ion bombardment at not-too-large energies. More quantitatively, the light-ion energy E should be smaller than

$$E < E_{\text{th}} \Big/ \frac{4M_i M_t}{(M_i + M_t)^2} , \tag{20}$$

where M_i (M_t) is the mass of the ion (target atom) and E_{th} is the threshold energy for kinetic electron emission of a target atom. This criterion is somewhat too severe, since target atoms recoiling with energy (20) will run *into* the target and hence do not immediately contribute to kinetic electron emission. The situation where recoil atoms do contribute to kinetic electron emission will be discussed further in Sec. IV C.

(v) Multiplication of electrons in electron cascades is neglected. This restricts the validity of our approach to low bombarding energies.

Comparison to experiment

The secondary electron emission statistics has been measured experimentally for $H^+ \rightarrow$Au.[9–12] These data[9] are reproduced in Fig. 2 and Table I. For the bombardment energy of 1 keV, we used the data of Ref. 10, since these were obtained with an improved detector system.[23] We refrained from including the data measured for $E < 1$ keV, since here the contribution from potential-electron emission becomes increasingly important. At 1 keV and above, this contribution is less than around 20%.[10]

Figure 2 compares the measured data with the sum of Poisson distribution, Eq. (2). For calculating the latter, we took the ion reflection coefficient from Ref. 24 and fitted γ_0 and γ_1 according to Eqs. (17) and (18). It is seen that the sum of Poisson distribution fits the data within a few percent. As is well known[3,5,9,25] a single Poissonian fails to describe electron emission statistics. Often, the two-parameter Polya distribution is empirically used to describe the measured data. However, it has been pointed out that there is no theoretical basis for using Polya distributions in this context.[3] We note that, numerically, both the sum of Poisson and the Polya distributions describe the experimental data with comparable accuracy.

Table I lists the parameters describing the electron emission statistics induced by low-keV proton bombardment of Au surfaces. We observe that γ_0 and γ_1 increase with increasing ion-bombarding energy. This is plausible because the electron excitation cross section σ_x^+ (and σ_x^-) will increase with increasing energy. Also, γ_1 is larger than $2\gamma_0$ for all energies. This is sensible if we note that from Sec. II,

$$\frac{\gamma_1}{\gamma_0} = 1 + \frac{L_x^0}{L_x^+} = 1 + \frac{\sigma_x^+ + \sigma_x^- R_e}{\sigma_x^- + \sigma_x^+ R_e} , \tag{21}$$

which is larger than 2 for $\sigma_x^- < \sigma_x^+$.

We may attempt to extract further microscopic information on the electron excitation and transport mechanisms from the data. To this end, let us assume—as is often done—that the main mechanism of kinetic electron excitation consists in direct knock-on collisions of the ion with target valence electrons. In such collisions, the electron is excited in the *forward* direction with respect to the ion motion, i.e., $\sigma_x^- = 0$.[3,14,15,26] With this simplification, we learn that

$$R_e = \frac{\gamma_0}{\gamma_1 - \gamma_0} \tag{22}$$

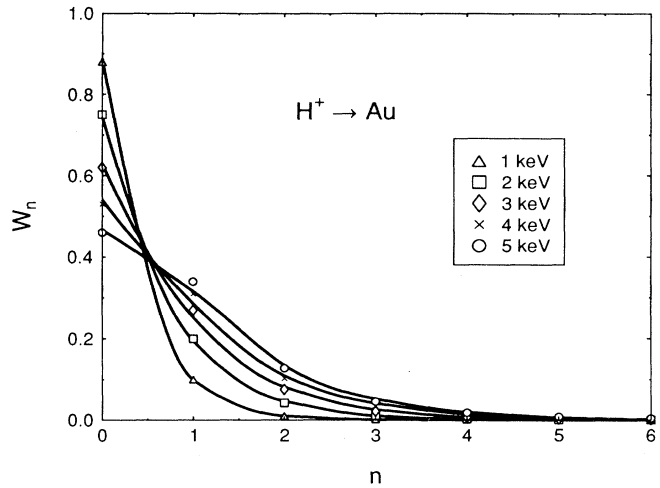

FIG. 2. Comparison of experimental and theoretical results on the statistics of electron emission induced by keV H^+ ion bombardment of Au. Symbols, experimental data (Refs. 9 and 10): Lines, calculated data, using Eq. (2) and Table I. Calculated data W_n have been smoothly splined in order to enhance readability.

TABLE I. Parameters describing the statistics of kinetic electron emission induced by energetic H^+ ions bombarding a Au surface with energy E. Experimental data (Refs. 9 and 10) of the average yield γ and the variance σ^2, as well as of the ion reflection coefficient (Ref. 24) R. Parameters γ_0 and γ_1 calculated from Eqs. (17) and (18).

E (keV)	γ	σ^2	R	γ_0	γ_1
1	0.124	0.136	0.38	0.037	0.266
2	0.331	0.409	0.32	0.139	0.739
3	0.537	0.708	0.28	0.279	1.200
4	0.724	0.990	0.26	0.418	1.594
5	0.873	1.151	0.24	0.577	1.812

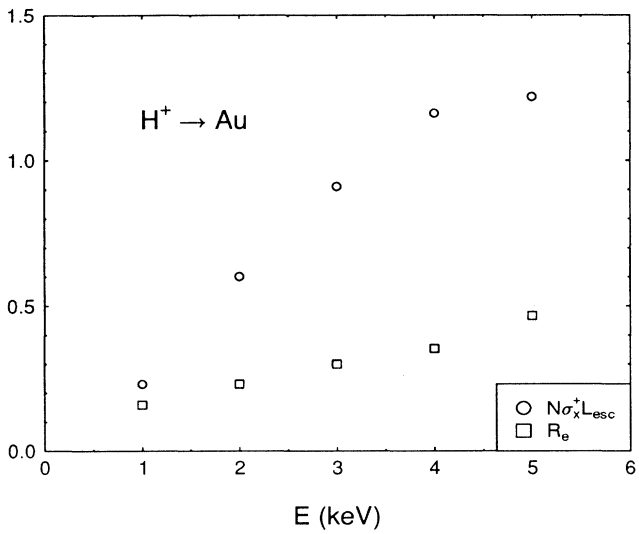

FIG. 3. Electron reflection coefficient R_e (□) and dimensionless forward excitation cross section $N\sigma_x^+ L_{\rm esc}$ (○) for H^+ bombardment of energy E of Au. Experimental data (Refs. 9 and 10), as given in Table I, interpreted according to Eqs. (22) and (23).

and

$$N\sigma_x^+ L_{\rm esc} = \gamma_1 - \gamma_0 \ . \tag{23}$$

These expressions give us a new interpretation of direct microscopic interest of the joint average yields γ_0 and γ_1.

Figure 3 displays an analysis of the experimental data (cf. Table I). It is seen that $N\sigma_x^+ L_{\rm esc}$ increases steadily with bombarding energy. Even though $L_{\rm esc}$ will show some intrinsic energy dependence itself—according to Eq. (11) the electron escape length presumably increases with energy in metals—it may be assumed that the dominant energy dependence stems from σ_x^+, as the data refer to energies just above threshold. The kinematical threshold for kinetic electron emission of H^+ in Au is around 300 eV. The electron reflection coefficient shows also a monotonous, but softer, increase with energy; this is plausible.

IV. EXTENSIONS

A. Generalization to nonstraight ion trajectory

Up to now, we have disregarded the details of the ion motion in the target. That is, we assumed an essentially straight ion trajectory in the escape depth $L_{\rm esc}$ of the electrons. This is certainly not a bad approximation, but may not appear entirely consistent, since after all, ion reflection in the target has been incorporated via the ion reflection coefficient R. In this section we briefly present how ion transport can be incorporated consistently in the invariant-embedding approach of Sec. II. This will allow us to discuss quantitatively some of the limitations of the sum of Poisson model.

In analogy to the elastic- ($\sigma_{\rm el}$) and inelastic- ($\sigma_{\rm in}$) scattering cross sections of the electrons, we introduce the ion elastic- and inelastic-scattering cross sections $\Sigma_{\rm el}$ and $\Sigma_{\rm in}$. We list in Fig. 4 those processes which have to be taken into account for an invariant-embedding analysis of electron emission, in addition to the processes of Fig. 1. From the invariant-embedding analysis, we hence obtain

$$0 = \frac{n+1}{L_{\rm esc}} W_{n+1}^0 - \left[\frac{1}{L_x^0} + \frac{n}{L_{\rm esc}} + \frac{1}{L_{\rm in}} + \frac{1}{L_{\rm el}} \right] W_n^0 + \frac{1}{L_x^0} W_{n-1}^0 + \frac{1}{L_{\rm in}} W_n^1 + \frac{1}{L_{\rm el}} \sum_{m=0}^{n} W_m^1 W_{n-m}^0 + \frac{1}{L_{\rm in}} \delta_{n0} \tag{24}$$

and

$$0 = \frac{n+1}{L_{\rm esc}} W_{n+1}^1 - \left[\frac{1}{L_x^1} + \frac{n}{L_{\rm esc}} + \frac{2}{L_{\rm in}} + \frac{2}{L_{\rm el}} \right] W_n^1 + \frac{1}{L_x^1} W_{n-1}^1 + \frac{1}{L_{\rm el}} \sum_{m=0}^{n} W_m^1 W_{n-m}^1 + \frac{1}{L_{\rm el}} \delta_{n0} \ . \tag{25}$$

Here, $1/L_{\rm in} = N\Sigma_{\rm in}$, $1/L_{\rm el} = N\Sigma_{\rm el}$, and δ_{n0} is the Kronecker symbol. We note that the improved representation of the ion trajectory renders the equations nonlinear and inhomogeneous, unlike the simple model of Eq. (9). Equations (24) and (25) are not solved by Poisson distributions. In the limit $L_{\rm in}$, $L_{\rm el} \to \infty$, our old result, the sum of Poisson model, is recovered. We furthermore note that the equations describing W_n^0 and W_n^1 are now coupled.

Equation (25) allows us to calculate the ion reflection coefficient R. Summing Eq. (25) over all n and employing the normalization (15), we obtain

$$R^2 - 2\left[1 + \frac{L_{\rm el}}{L_{\rm in}}\right] R + 1 = 0 \ . \tag{26}$$

process	+gain / −loss to W_n^0	+gain / −loss to W_n^1
vacuum Δx target		
	$+N\Sigma_{\rm in}\Delta x\delta_{n0}$ $-N\Sigma_{\rm in}\Delta x W_n^0$	$+0$ $-N\Sigma_{\rm in}\Delta x W_n^1$
	$+0$ $-N\Sigma_{\rm el}\Delta x W_n^0$	$+N\Sigma_{\rm el}\Delta x\delta_{n0}$ $-N\Sigma_{\rm el}\Delta x W_n^1$
	$+N\Sigma_{\rm in}\Delta x W_n^1$ -0	$+0$ $-N\Sigma_{\rm in}\Delta x W_n^1$
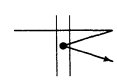	$+N\Sigma_{\rm el}\Delta x \sum_{m=0}^{n} W_m^1 W_{n-m}^0$ -0	$+N\Sigma_{\rm el}\Delta x \sum_{m=0}^{n} W_m^1 W_{n-m}^1$ $-N\Sigma_{\rm el}\Delta x W_n^1$

FIG. 4. Processes contributing in the invariant-embedding analysis of electron emission, if ion scattering and stopping, with cross sections $\Sigma_{\rm el}$ and $\Sigma_{\rm in}$, are taken into account (Sec. IV A). This list uses the same notation as Fig. 1, which it complements.

Hence the ion reflection coefficient R can be expressed by the ratio of the ion elastic- and inelastic-scattering lengths

$$R=1+\frac{L_{\rm el}}{L_{\rm in}}-\left[\frac{L_{\rm el}}{L_{\rm in}}\left[\frac{L_{\rm el}}{L_{\rm in}}+2\right]\right]^{1/2} . \tag{27}$$

This shows that the improved description of the ion trajectory, Eqs. (24) and (25), introduces only one further parameter as compared to Eq. (9), viz., the ratio of a scattering length of the ion versus that of an electron. We note that the electron reflection coefficient R_e obeys a relationship analogous to Eq. (27) [cf. Eq. (19)].

Equations (24) and (25) may be solved iteratively. The solution is achieved using a shooting technique. Consider first Eq. (25) since it is uncoupled from Eq. (24). A starting value for W_0^1 is chosen and W_1^1, W_2^1, etc., are calculated recursively from Eq. (25). If $W_n^1<0$ for some n or if $\sum_{m=0}^{n} W_m^1>1$, the recursion is restarted with an adequately modified starting value W_0^1. This is repeated until the correct value for W_0^1, and hence all W_n^1, is found. Then, Eq. (24) is solved analogously. We found that this solution scheme converges quickly, even for grossly wrong starting values of W_0^1.

We now present results in order to illustrate the effect of fluctuations of the ion trajectory within the escape depth $L_{\rm esc}$ of the electrons. To this end, we keep the electron length scales fixed, including the excitation lengths L_x^0 and L_x^1. We also fix the ratio $L_{\rm el}/L_{\rm in}$ by setting $R=0.25$, and vary only the parameter $\lambda=\Sigma_{\rm in}/\sigma_{\rm in}$, i.e., the ion stopping length $L_{\rm in}$. For $\lambda\to 0$, we thus recover the sum of Poisson model.

Figure 5 shows the electron distribution for $\lambda=0.01$, 0.1, and 1. A noticeable influence is only seen for $\lambda=1$, i.e., when the ion range becomes comparable to the electron range. In this case, the probability W_0 that no electrons are emitted is increased. Hence, the average yield γ decreases if the ion length scale becomes comparable to the electron scale. This is because the ion may stop shortly after entering the target.

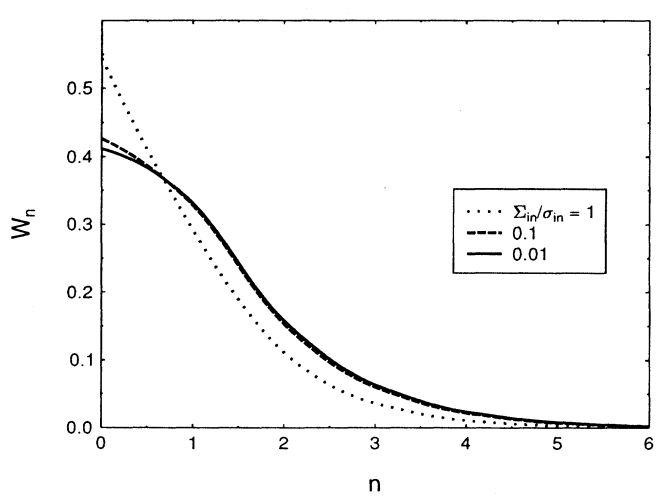

FIG. 5. Influence of ion stopping cross section $\Sigma_{\rm in}$ on electron emission statistics W_n. Results calculated from Eqs. (24) and (25). The parameters are chosen as $R=0.25$, $R_e=0.58$, $\sigma_x^-=0$, and $N\sigma_x^+L_{\rm in}=4.53$. Calculated data W_n have been smoothly splined in order to enhance readability.

In reality, however, keV protons have ranges of the order of several 100 Å, whereas the secondary electrons have ranges of several 10 Å only,[27] and thus in practice $\lambda\cong 0.1$. Thus, we may conclude that Fig. 5 validates the simplified concept of a sum of Poisson distribution. We note that the situation might be different, however, for the case of grazing ion incidence.

B. Energy dependence

On its way through the target, the ion loses energy. Hence, when it is reflected towards the surface, it will have less energy to excite electrons there. This energy dependence of the ion can be crucial for near-threshold kinetic electron-emission processes. It can be included in the analysis in a straightforward manner, if we ignore the ion scattering in the layer $L_{\rm esc}$ as in Sec. II. Note first that the contribution W_n^0 does not change, since the incoming ion trajectory is unaffected within $L_{\rm esc}$ by energy loss. Let E_0 be the bombarding energy and let us furthermore denote by $W_n^1(E)dE$ the joint probability that n electrons are emitted *and* the ion is reflected towards the surface with an energy between E and $E+dE$. We have the normalization

$$\sum_{n=0}^{\infty} W_n^1(E)=R(E) , \tag{28}$$

where the energy distribution of reflected ions, $R(E)$, obeys

$$\int R(E)dE=R . \tag{29}$$

A balance equation in strict analogy to Eq. (9) can be set up for $W_n^1(E)$. Including explicitly the energy of the ion at the electron excitation process in the cross sections $\sigma_x^{+,-}$, we obtain an equation of the form (9) with an ion-energy-dependent excitation length

$$L_x^1(E)=1/N\{\sigma_x^-(E_0)+\sigma_x^+(E)+R_e[\sigma_x^-(E)+\sigma_x^+(E_0)]\} . \tag{30}$$

Hence, the electron-emission statistics reads

$$\begin{aligned} W_n&=W_n^0+\int dE\, W_n^1(E)\\ &=(1-R)P_n(\gamma_0)+\int dE\, R(E)P_n[\gamma_1(E)] , \end{aligned} \tag{31}$$

where

$$\gamma_1(E)=L_{\rm esc}/L_x^1(E) . \tag{32}$$

This distribution is again of a sum of Poisson form.

Let us consider the case that reflected ions have such a low energy that the excitation cross sections $\sigma_x^{+,-}(E)$ are negligibly small. Then it is $L_x^1(E)=L_x^0$, and we recover

$$W_n=P_n(\gamma_0) , \tag{33}$$

which is obvious in this case.

One might wish to include as well the energy dependence of the electron scattering cross sections σ_{el} and σ_{in} and consequently of the electron reflection coefficient R_e. In the present framework, this would necessitate considering the probabilities

$$W_n^{0,1}(E_1,\ldots,E_n)dE_1\ldots dE_n$$

of emitting exactly n electrons with their energies in the specified energy windows. While a set of integral equations can be readily written up with the methods of Sec. II, their solution is highly nontrivial. Moreover, the information contained in these quantities is far more complex than the existing experimental data. We therefore do not consider electron energy dependence any further. It appears that Monte Carlo simulations of the type reported in Refs. 22, 28, and 29 are best suited to this purpose.

C. Recoil contribution

At higher bombarding energy or higher ion mass, the ion may create target recoil atoms with energies sufficiently high to contribute to electron emission. While, for light-ion bombardment at energies not too far above threshold, such a recoil contribution to electron emission will be small, it may contribute substantially in the case of heavier ions.[16]

Modeling the recoil contribution using the above methods hardly appears possible. Tentatively, we might argue as follows: Let the probability of finding exactly m recoils with sufficient energy in a surface layer of thickness L_{esc} be denoted by R_m, such that $\sum_m R_m = 1$. Let us furthermore denote the average electron yield for a cascade with m such recoils by γ_m. Then, in analogy to Eq. (2), it is

$$W_n = \sum_m R_m P_n(\gamma_m) \ . \tag{34}$$

The average electron yield is given by

$$\langle n \rangle = \sum_m R_m \gamma_m \ , \tag{35}$$

and the variance reads

$$\sigma^2 = \langle n^2 \rangle - \langle n \rangle^2 = \sum_{l>m} R_l R_m (\gamma_l - \gamma_m)^2 + \sum_m R_m \gamma_m > \langle n \rangle \ . \tag{36}$$

As in Eq. (18), the electron distribution is broader than in a single Poissonian: Cascade fluctuations add to electron fluctuations. Decisive for the extra broadening of the electron-emission statistics is the recoil statistics, i.e., the distribution of the number of recoils passing a layer extending one electron escape length L_{esc} from the surface with sufficient energy to excite electrons. Such a recoil statistics is not available. It is known, however, that the total number of recoils created anywhere in the cascade shows only small, i.e., sub-Poissonian, fluctuations.[30] On the other hand, the distribution of recoils created very close to the surface, within the sputter depth, is very broad such that its variance is of the same order of magnitude as its average.[31] The recoil statistics we are looking for is intermediate between these two.

V. CONCLUSIONS

(1) The statistics of light-ion-induced kinetic electron emission can be explained via a sum of Poisson model. It makes use of the fact that the ion is either stopped or reflected. In both cases it emits electrons with a Poisson distribution. The weight with which each Poisson term enters the distribution depends on the ion reflection coefficient.

(2) A quantitative formulation can be obtained within the invariant-embedding approach to the transport of ions and electrons in the solid. We include angular scattering and stopping, electron excitation, and elastic and inelastic scattering of the electrons. The sum of Poisson distribution results if the ion trajectory changes on a much larger scale than the electron trajectories, and hence can be assumed to be a straight line in the vicinity of the surface. We check the influence of a more realistic inclusion of the ion trajectory on the electron emission statistics. Allowing for ion scattering and stopping in the electron escape depth leads to deviations of the electron statistics from the sum of Poisson form. For a realistic example, quantitative changes are small.

(3) In our model, the electron statistics is broader than a single Poisson distribution. It is determined by three parameters, viz., the ion reflection coefficient, and the average electron yields of the ion when it is stopped in the target, or reflected from the target. We present analytical formulas which express these parameters in terms of the microscopic scattering and stopping cross sections of the excited electrons in the target.

(4) Comparison to experimental data is favorable. Electron emission statistics data may be used to gain information on microscopic parameters for electron excitation and transport in solids.

(5) The model may in principle be extended to heavier ion bombardment and higher energies by including kinetic electron emission due to energetic recoil atoms. As a consequence of the additional sources of electron emission, the distribution broadens further.

ACKNOWLEDGMENTS

We thank F. Aumayr and H. Winter for drawing our attention to this problem, and U. Conrad for discussions.

[1] *Particle Induced Electron Emission I,* with contributions by M. Rösler, W. Brauer, J. Devooght, J.-C. Dehaes, A. Dubus, M. Cailler, and J.-P. Ganachaud, Springer Tracts in Modern Physics Vol. 122 (Springer, Berlin, 1991).

[2] *Particle Induced Electron Emission II,* with contributions by D. Hasselkamp, H. Rothard, K.-O. Groeneveld, J. Kemmler, P. Varga, and H. Winter, Springer Tracts in Modern Physics Vol. 123 (Springer, Berlin, 1992).

[3] W. O. Hofer, Scanning Microsc. Suppl. **4**, 265 (1990).

[4] J. Schou, Scanning Microsc. **2**, 607 (1988).

[5]P. Sigmund, in *Ionization of Solids by Heavy Particles, NATO Advanced Study Institute, Series B: Physics,* edited by R. A. Baragiola (Plenum, New York, in press).
[6]F. Bernhard, K. H. Krebs, and I. Rotter, Z. Phys. **161**, 103 (1965).
[7]C. F. G. Delaney and P. W. Walton, IEEE Trans. Nucl. Sci. **NS-13**, 742 (1966).
[8]G. Staudenmaier, W. O. Hofer, and H. Liebl, Int. J. Mass Spectrom. Ion Phys. **11**, 103 (1976).
[9]G. Lakits, F. Aumayr, and H. Winter, Rev. Sci. Instrum. **60**, 3151 (1989).
[10]G. Lakits, F. Aumayr, M. Heim, and H. Winter, Phys. Rev. A **42**, 5780 (1990).
[11]F. Aumayr, G. Lakits, and H. Winter, Appl. Surf. Sci. **47**, 139 (1991).
[12]H. Winter, F. Aumayr, and G. Lakits, Nucl. Instrum. Methods B **58**, 301 (1991).
[13]E. J. Sternglass, Phys. Rev. **108**, 1 (1957).
[14]R. A. Baragiola, E. V. Alonso, and A. Oliva-Florio, Phys. Rev. B **19**, 121 (1979).
[15]R. A. Baragiola, E. V. Alonso, J. Ferron, and A. Oliva-Florio, Surf. Sci. **90**, 240 (1979).
[16]J. Schou, Phys. Rev. B **22**, 2141 (1980).
[17]P. Sigmund and S. Tougaard, in *Inelastic Particle-Surface Collisions,* edited by E. Taglauer and W. Heiland, Springer Series in Chemical Physics Vol. 17 (Springer, Berlin, 1981), p. 2.
[18]S. Tougaard and P. Sigmund, Phys. Rev. B **25**, 4452 (1982).
[19]V. A. Ambarzumian, Russ. Astronom. J. **19**, 1 (1942).
[20]S. Chandrasekhar, *Radiative Transfer* (Oxford University Press, London, 1950).
[21]M. Wing, *An Introduction to Transport Theory* (Wiley, New York, 1962).
[22]K. Ohya, F. Aumayr, and H. Winter, Phys. Rev. B **46**, 3101 (1992).
[23]F. Aumayr (private communication).
[24]T. Tabata, R. Ito, K. Morita, and H. Tawara, Nucl. Instrum. Methods B **9**, 113 (1985).
[25]L. A. Dietz and J. C. Sheffield, J. Appl. Phys. **46**, 4361 (1975).
[26]D. Hasselkamp, in *Particle Induced Electron Emission II* (Ref. 2), p. 1.
[27]M. E. Riley, C. J. MacCallum, and F. Briggs, At. Data Nucl. Data Tables **15**, 443 (1975).
[28]J. Kawata, K. Ohya, and I. Mori, Jpn. J. Appl. Phys. **30**, 3510 (1991).
[29]K. Ohya and I. Mori, Nucl. Instrum. Methods B **67**, 628 (1992).
[30]G. Leibfried, Nukleonik **1**, 57 (1958).
[31]U. Conrad and H. M. Urbassek, Nucl. Instrum. Methods B **48**, 399 (1990).